

SCHRÖDINGER'S RADIAL EQUATION: SOLUTION BY EXTRAPOLATION

D. GOORVITCH† and D. C. GALANT‡

†Space Sciences Division and ‡Information Systems Division, NASA Ames Research Center,
Moffett Field, CA 94035, U.S.A.

(Received 22 August 1991)

Abstract—Combining an appropriate finite difference method with iterative extrapolation to the limit results in a simple, highly accurate, numerical method for solving a one-dimensional Schrödinger's equation appropriate for a diatomic molecule. This numerical procedure has several distinct advantages over the more conventional methods such as Numerov's method or the method of finite differences without extrapolation. The advantages are the following: (i) initial guesses for the term values are not needed; (ii) the algorithm is easy to implement, has a firm mathematical foundation and provides error estimates; (iii) the method is relatively less sensitive to round-off error since a small number of mesh points is used and, hence, can be implemented on small computers; (iv) the method is faster for equivalent accuracy. We demonstrate the advantages of the present algorithm by solving Schrödinger's equation for (a) a Morse potential function appropriate for HCl and (b) a numerically derived Rydberg–Klein–Rees potential function for the $X^1\Sigma^+$ state of CO. A direct comparison of the results for the $X^1\Sigma^+$ state of CO is made with results obtained using Numerov's method.

INTRODUCTION

Radiation from diatomic molecules plays a key role in the solution of many important problems. For instance, a critical ingredient in solving the equation of radiative transfer for a stellar atmosphere is the intrinsic opacity of the constituent molecules. However, observed spectral features are significantly modified by their environment. Knowledge of the intrinsic spectral properties of the emitting species is necessary to unravel the chemical and physical state of a stellar atmosphere.¹ Usually, the transition frequencies can be calculated very accurately using a matrix formulation of the Hamiltonian that includes several interacting states. Equally important is knowledge of the strength of the transitions. The strength of a diatomic transition depends upon an accurate expectation value for the transition moment. For electronic transitions, an additional requirement is the Franck–Condon factor, which is the square of the vibrational overlap integral.

In measurements of the transition strengths, the square of the dipole transition moment is observed. Deducing the electric dipole moment function (EDMF) from observations of the transition strengths depends critically on the wavefunctions of the states involved in the observed transitions.² Once the functional dependence of the EDMF is deduced, calculation of all the transitions in a system and the Franck–Condon factors depends upon accurate wavefunctions.

Given a potential function for a diatomic molecule, the wavefunctions can be calculated by numerically solving a 1-D radial Schrödinger equation.^{3,4} The Rydberg–Klein–Rees (RKR) method is a popular method of obtaining the molecular potential function of a diatomic molecule from observations of its term values.⁵ The RKR method with a second-order correction gives the potential curve turning points from the measured vibrational energies, G_v , and the rotational constants, B_v , where v is the vibrational quantum number. A 1-D Schrödinger equation is usually solved numerically by one of two methods. The first is to solve Schrödinger's equation using the Numerov algorithm,³ while the second employs an alternate finite difference method.^{6,7} Both methods give identical results if a sufficient number of mesh points are used.

However, the number of mesh points needed to obtain sufficient accuracy may be rather large ($n \approx 6000$ points). The matrix finite difference method then leads to large matrices for which eigensolutions are needed. Numerov's method also is susceptible to overflows in calculating the wavefunctions.

The Numerov method is of the fourth order while the matrix method is second order. Both are flexible for determining blocks of selected levels of v , the matrix method because there are stock numerical methods available for finding any contiguous block of eigensolutions and the method is easily modified to find all the eigensolutions between two values of v .⁸

The results of the matrix method are easily improved using Richardson's extrapolation and can be used to obtain results of very high accuracy on relatively coarse meshes.⁹⁻¹¹ Furthermore, fairly accurate *a posteriori* error estimates are available and can be used either to bound the error of the calculated results or to control the computation to achieve a preselected accuracy. Richardson's extrapolation can be applied pointwise to the wavefunctions so that wavefunctions with precise error bounds on coarse meshes are available. Precise error bounds are not easily available for the Numerov method and a very fine mesh may be necessary to achieve a given accuracy. Numerical problems from computational error may degrade the results.

With these possible limitations in mind, we have developed an algorithm based upon Richardson's iterative extrapolation to a limit.⁹⁻¹¹ This method gives high accuracy when using a small number of mesh points, thereby reducing storage requirements and diminishing the computational time required. We have successfully run this algorithm on an IBM-compatible DOS computer with 640 kbytes of available memory. This method also yields simple *a posteriori* estimates of the errors in the derived wavefunctions and energy levels. Additionally, initial guesses for the term values are not needed, and the algorithm is easy to implement. The method is also less sensitive to round-off error and is not susceptible to overflows in calculating accurate eigenfunctions as is Numerov's method. An additional advantage of the present method is that the slopes of the wavefunctions near the end points of the interval of integration are not needed.

METHOD

Many methods have been proposed for solving the second-order differential equation

$$-\frac{d^2y}{dx^2} + D(x) \frac{dy}{dx} + [V(x) - E]y = 0, \quad (1)$$

with the boundary conditions $y(a) = y(b) = 0$ and $a \leq x \leq b$. When $D(x) = 0$, this is Schrödinger's equation, with $V(x)$ being the potential energy of the system and E the energy in dimensionless units. Replacement of the derivatives with the simple finite difference approximations

$$\frac{d^2f(x)}{dx^2} = \frac{f(x+h) - 2f(x) + f(x-h)}{h^2} \quad (2)$$

and

$$\frac{df(x)}{dx} = \frac{f(x-h) - f(x+h)}{2h}, \quad (3)$$

which have the error expansions

$$-2 \sum_{k=1}^m \frac{f^{(2k+2)}(x)}{(2k+2)!} h^{2k} + \mathcal{O}(h^{2m+1}) \quad (4)$$

and

$$-\sum_{k=1}^m \frac{f^{(2k+1)}(x)}{(2k+1)!} h^{2k} + \mathcal{O}(h^{2m+1}), \quad (5)$$

respectively, changes the differential equation to the system of linear equations

$$\mathbf{A}\phi = (Eh^2)\phi, \quad (6)$$

where the matrix $\mathbf{A} = \text{tridiagonal}\{-1 + D(x_i)h/2, 2 + V(x_i)h^2, -1 - D(x_i)h/2\}$ and $\phi^i = \phi(x_i)$, $h = (b-a)/N$ is the mesh size and N the number of mesh points, $V(x_i)$ is the molecular potential function, $x_i = ih$, E is the eigenvalue and ϕ the eigenfunction. If we choose the step size $h < 2/\max|D(x)|$, where $a \leq x \leq b$, then only real solutions exist and these equations can be solved

for the eigensolutions (E_i and ϕ^i) using standard techniques for symmetrizing tridiagonal matrices and then using standard techniques like TSTURM for symmetric tridiagonal matrices to compute the eigenvalues and eigenvectors in a given interval by Sturm sequencing.⁸

If the potential function in Schrödinger's equation is piecewise differentiable up to order $2m + 1$, then both the eigenvalues, E_i , and eigenfunctions, ϕ^i , of Eq. (6) have error expansions, viz.

$$E_i(h) = E_i + \sum_{n=1}^m c_n(i)h^{2n} + \mathcal{O}(h^{2m+1}) \quad (7)$$

and

$$\phi^i(h) = \phi(x_i) + \sum_{n=1}^m \chi_n(i)h^{2n} + \mathcal{O}(h^{2m+1}), \quad (8)$$

where $i = 1, 2, \dots$ and $c_n(i)$ and the $\chi_n(i)$ are independent of the mesh size h .¹²

By properly combining solutions on meshes of different sizes, we obtain highly accurate eigenvalues and eigenfunctions on the points of the crudest mesh. This approach is often called Richardson's extrapolation.^{10,13} It involves interpolating a polynomial through the points $[h^2, f(h)]$, $[(h/2)^2, f(h/2)]$, \dots , $[(h/2^n)^2, f(h/2^n)]$ and evaluating this polynomial at 0. This is easily done using Neville's algorithm for linear iterative interpolation to generate a table from the rules

$$T_m^{(k)} = T_{m-1}^{(k+1)} + \frac{T_{m-1}^{(k+1)} - T_{m-1}^{(k)}}{4^m - 1}, \quad (9)$$

$k = 1, 2, \dots$, and $m = 1, 2, \dots, k$;¹⁴ the starting conditions are $T_0^{(k)} = E_i(h/2^k)$ for the i th eigenvalue and $T_0^{(k)} = \phi_{j2^k}^i(h/2^k)$ at the j th mesh point of the i th eigenfunction. For fixed m , the elements $T_m^{(k)}$ have error expansions in even powers of h and are all $\mathcal{O}(h^{2m+1})$. Since $\lim_{k \rightarrow \infty} T_m^{(k)} = T(0)$, a very simple asymptotic estimate of the error $R_m^{(k)}$ in $T_m^{(k)}$ is¹⁵

$$R_m^{(k)} \approx -\frac{T_m^{(k+1)} - T_m^{(k)}}{4^{m+1} - 1}. \quad (10)$$

The table calculation can be organized by rows, so that the error estimation may be done simultaneously. Thus, the process can be stopped when an error criterion has been met or after a predetermined maximum number of extrapolations. Only the last row of the table and the new estimate are required for the next row of the table. The index m denotes the order of the extrapolation while $k = 1, 2, \dots$ denote the mesh sizes. Thus, for a third-order extrapolation, $m = 3$ and Eq. (6) is evaluated at mesh sizes h , $h/2$, $h/4$, and $h/8$. An example of a third-order extrapolation is given in Table 1. We then have the following set of equations for each l th eigenvalue:

$$\begin{aligned} E_1^1(h) &= E_1^0(h/2) + [E_1^0(h/2) - E_1^0(h)]/3, \\ E_1^1(h/2) &= E_1^0(h/4) + [E_1^0(h/4) - E_1^0(h/2)]/3, \\ E_1^1(h/4) &= E_1^0(h/8) + [E_1^0(h/8) - E_1^0(h/4)]/3, \\ E_2^2(h) &= E_1^1(h/2) + [E_1^1(h/2) - E_1^1(h)]/15, \\ E_2^2(h/2) &= E_1^1(h/4) + [E_1^1(h/4) - E_1^1(h/2)]/15, \\ E_3^3(h) &= E_2^2(h/2) + [E_2^2(h/2) - E_2^2(h)]/63; \end{aligned} \quad (11)$$

Table 1. Terms $T_m^{(k)}$ for a third-order extrapolation energy E_i .

$k \backslash m$	0	1	2	3		0	1	2	3
0	$T_0^{(0)}$					$E_i^0(h)$			
1	$T_0^{(1)}$	$T_1^{(0)}$				$E_i^0(h/2)$	$E_i^1(h)$		
2	$T_0^{(2)}$	$T_1^{(1)}$	$T_2^{(0)}$			$E_i^0(h/4)$	$E_i^1(h/2)$	$E_i^2(h)$	
3	$T_0^{(3)}$	$T_1^{(2)}$	$T_2^{(1)}$	$T_3^{(0)}$	\rightarrow	$E_i^0(h/8)$	$E_i^1(h/4)$	$E_i^2(h/2)$	$E_i^3(h)$

the asymptotic estimates of the errors for each order of extrapolation are given by

$$\begin{aligned}
 R_1^{(0)} &= -[E_l^0(h/2) - E_l^0(h)]/15, \\
 R_1^{(1)} &= -[E_l^0(h/4) - E_l^0(h/2)]/15, \\
 R_1^{(2)} &= -[E_l^0(h/8) - E_l^0(h/4)]/15, \\
 R_2^{(0)} &= -[E_l^1(h/2) - E_l^1(h)]/63, \\
 R_2^{(1)} &= -[E_l^1(h/4) - E_l^1(h/2)]/63, \\
 R_3^{(0)} &= -[E_l^2(h/2) - E_l^2(h)]/255.
 \end{aligned} \tag{12}$$

A set of equations similar to Eqs. (11) and (12) will give the third-order extrapolation for each l th eigenfunction, $\phi_l^3(h)$.

Of course, one usually calculates wavefunctions as a step toward calculating expectation values, line strengths, or other integrals. These integrals are surprisingly easy to calculate accurately from the finite difference wavefunctions; it is not even necessary to extrapolate wavefunctions to achieve the desired accuracy.

As we have noted, the eigenvectors from the finite difference approximation have pointwise errors which are given by series in h^2 . Thus, any numerical approximation to an integral which uses these wavefunctions also has such an expansion, no matter what the intrinsic error expansion of the numerical integration method. The trapezoidal rule approximation to an integral also has an error which is a series in h^2 . Thus, using the trapezoid-rule approximation and the unextrapolated wavefunctions for the integrals leaves the error as a series in h^2 . These approximations can be extrapolated to get an accurate estimate of the integral, which is considerably faster and easier to do than extrapolating the wavefunctions and then evaluating the integral, and have the additional advantage of allowing the error to be estimated.

We are interested only in the bounded states or, at most, in a small number of continuum states. Therefore, we only need to solve for the first M eigenstates, usually corresponding to the lowest 50 energy levels. The smallest number of mesh points for which the estimates of the eigenfunctions are valid seems to be about 4 values per oscillation. For the fiftieth eigenfunction, the number of oscillations is 49 and, thus, the minimum number of mesh points is about 200. Because extrapolation method requires a coarser mesh than other methods for a given accuracy, the method we propose is less sensitive to roundoff error, although this sensitivity also depends upon the accuracy of the arithmetic.

With L coupled Schrödinger equations, the error expansions retain the form given by Eqs. (7) and (8). This numerical method may therefore be extended to the coupled case. The only difference is that the matrix \mathbf{A} in Eq. (6) is no longer tridiagonal but has the width $2L + 1$ instead.¹⁶

While the number of points in a submesh increases exponentially, few extrapolations are necessary in practice and, on the average, the method uses only about half the number of mesh points required for methods based upon integration of the differential equations with Numerov's method. Furthermore, if the eigenfunction values are not required, then submeshes can be chosen so that the number of points increases far more slowly. Roundoff error plays a lesser role in the present method than for other methods because the number of mesh points is reduced and all of the numerical processes used are stable.

The accuracy of the derived wavefunctions can be estimated by calculating the rotational constant for each vibrational state, using

$$B_v = \int_{r_{\min}}^{r_{\max}} r^{-2} |\Psi_v(r)|^2 dr. \tag{13}$$

The integration limits (r_{\min}, r_{\max}) are chosen so that the contribution to B_v of the integral outside these limits is negligible. The value given by Eq. (13) can then be compared with the value for B_v derived experimentally.

CALCULATIONS

We test our algorithm and demonstrate its advantages by using both an analytical and a numerical potential function. The analytical potential function chosen is the Morse potential function appropriate for HCl while, for the numerically-derived potential, an RKR potential function derived from observations of the $X^1\Sigma^+$ state of CO is used.

(a) The analytical potential function

The parameters appropriate for HCl are taken from the paper by Cashion.¹⁷ Cashion gives for the Morse potential function

$$V(x) = D_\infty [1 - e^{-\beta(x-x_e)}]^2, \quad (14)$$

where the dissociation energy $D_\infty = 605.559$, the equilibrium internuclear distance $x_e = 2.40873$, and $\beta = 0.988879$, all dimensionless. The dimensionless energy levels, E_v , and the rotational constants, B_v , can be calculated from these parameters using

$$E_v = \omega_e(v + 1/2) - \omega_e x_e(v + 1/2)^2, \quad (15)$$

$$B_v = B_e - \alpha_e(v + 1/2) + \gamma_e(v + 1/2)^2 + \dots, \quad (16)$$

where

$$\omega_e = 2\beta\sqrt{D_\infty}, \quad (17)$$

$$\omega_e x_e = \beta^2, \quad (18)$$

$$B_e = r_e^{-2}, \quad (19)$$

$$\alpha_e = [3/(2\beta^2\sqrt{D_\infty})][\beta - 1/r_e], \quad (20)$$

$$\gamma_e = [3/(2\beta^2 r_e^6 D_\infty)][5 - 10r_e\beta + 23r_e^2\beta^2/4]. \quad (21)$$

Table 2 is a summary of the results of a second-order extrapolation using the Morse potential function for HCl.¹⁷ The columns in this table are, beginning from the left, the vibrational quantum

Table 2. Results for HCl with a Morse potential function; the superscripts have the following meaning: a refers to $1 - E_v^2(h)/E_v^{\text{Morse}}$, for b, B_v is calculated using Eq. (13); for c, $1 - B_v/B_v^{\text{Morse}}$.

v	$E_v^2(h)$ cm^{-1}	ΔE_v^a	B_v^b cm^{-1}	ΔB_v^c
0	1480.4214	4.80(-11)	10.43596867	5.58(-07)
1	4351.1224	2.28(-10)	10.12170596	1.19(-05)
2	7101.6342	7.28(-10)	9.80409410	4.66(-05)
3	9731.9568	1.72(-09)	9.48299513	1.21(-04)
4	12242.0902	3.34(-09)	9.15824910	2.58(-04)
5	14632.0344	5.71(-09)	8.82967774	4.84(-04)
6	16901.7894	8.91(-09)	8.49707471	8.33(-04)
7	19051.3552	1.29(-08)	8.16019399	1.35(-03)
8	21080.7318	1.79(-08)	7.81876390	2.09(-03)
9	22989.9192	2.36(-08)	7.47245173	3.14(-03)
10	24778.9173	3.02(-08)	7.12088691	4.58(-03)
11	26447.7262	3.74(-08)	6.76361279	6.56(-03)
12	27996.3459	4.52(-08)	6.40009765	9.23(-03)
13	29424.7764	5.33(-08)	6.02969801	1.28(-02)
14	30733.0176	6.16(-08)	5.65163797	1.76(-02)
15	31921.0697	6.98(-08)	5.26493705	2.41(-02)
16	32988.9326	7.76(-08)	4.86836942	3.29(-02)
17	33936.6063	8.47(-08)	4.46033863	4.48(-02)
18	34764.0909	9.08(-08)	4.03870919	6.13(-02)
19	35471.3863	9.54(-08)	3.60051382	8.43(-02)
20	36058.4927	9.83(-08)	3.14139120	1.17(-01)
21	36525.4099	9.90(-08)	2.67377300	1.59(-01)
22	36872.1380	9.71(-08)	2.12727961	2.40(-01)
23	37098.6782	6.35(-08)	1.55419637	3.57(-01)

number; the second-order extrapolation of the energy from Eq. (9) with $m = 2$ using meshes of 500, 1000 and 2000 points; one minus the ratio of the extrapolated energy from column 2 to the energy calculated from Eq. (15); the rotational constant calculated from Eq. (13) using the extrapolated eigenfunctions from Eq. (9); and one minus the ratio of the rotational constant calculated using Eq. (13) to the rotational constant calculated from the relationship given in Eq. (16). The difference between the extrapolated energies and the calculated energies is less than 1 part in 10^7 , as may be seen in column 3 of Table 2 and in Fig. 1. $R_2^{(0)}$ of Eq. (12) gives an estimate of the error. The estimated maximum error is 0.019 cm^{-1} for the $v = 19$ or about 5 parts in 10^7 . The actual error is about one-tenth of this. If we extend the outer potential limit, r_{\max} , we can calculate these levels to higher accuracy. The agreement between the rotational constants calculated by using the extrapolated wavefunctions and given by Eq. (16) vary from 6 parts in 10^7 to 0.3 as may be seen in column 5 of Table 2 and in Fig. 1. The large difference in rotational constants for high v results from neglecting higher terms in the expansion for B_v . The limits for r extend from 0.2 to 7.0 \AA in these calculations. Integrating from 0.2 to 4.0 \AA with meshes of 250, 500 and 1000 results in a degradation in the agreement for $v \geq 18$. This degradation is to be expected since we are approaching the dissociation limit for high v and the limits of integration need to be extended.

To make a direct comparison with the results of Cashion, who used a Numerov method with 1000 mesh points,¹⁷ we calculated values for E_v and B_v using meshes of 150, 300 and 600 points. Our results essentially agree with the results reported by Cashion for the first six vibrational levels, the highest level he calculated. Thus, we obtain results similar to those obtained for the Numerov method for the same number of total mesh points.

(b) The numerical potential function

As an additional test of our extrapolation algorithm, we replaced the analytical potential function by a numerically derived potential function. We chose the well studied results of a second-order semiclassical RKR calculation for the $X^1\Sigma^+$ state of CO.⁵ Using their RKR turning points to characterize the potential function for this state, we calculated the energy levels using

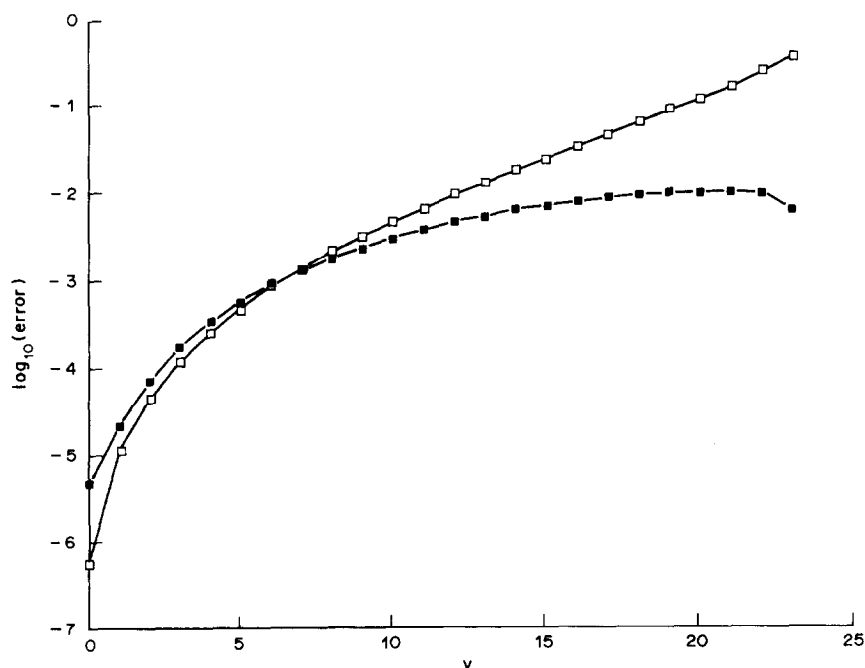


Fig. 1. The errors in term energies and rotational constants plotted as a function of vibrational quantum number for the Morse potential function results. The errors in the energy, ΔE_v , from column 3 of Table 2 are plotted as (■) after multiplying by 10^5 . The errors in the rotational constants, ΔB_v , from column 5 of Table 2 are plotted as (□).

Table 3. Results for the $X^1\Sigma^+$ state of $^{12}\text{C}^{16}\text{O}$; the superscripts have the following meanings: a refers to $E_v^2(h) - E_v^{\text{RKR}}$, for b, $E_v^{\text{Numerov}} - E_v^{\text{RKR}}$.

v	$E_v^2(h)$ cm^{-1}	ΔE_v^a cm^{-1}	E_v^{Numerov} cm^{-1}	ΔE_v^b cm^{-1}
0	1081.7653	-0.0138	1081.76644	-0.01266
1	3225.0100	-0.0422	3225.01105	-0.04115
2	5341.7735	-0.0702	5341.77270	-0.07101
3	7432.1231	-0.0969	7432.12369	-0.09632
4	9496.1261	-0.1233	9496.12554	-0.12386
5	11533.8522	-0.1491	11533.85061	-0.15069
10	21330.8798	-0.2671	21330.87761	-0.26930
15	30482.3212	-0.3689	30482.32131	-0.36882
20	38998.4345	-0.4472	38998.43679	-0.44494
25	46889.7457	-0.4649	46889.75761	-0.45303
30	54166.3696	-0.1236	54166.37660	-0.11664
35	60837.3172	1.7273	60837.23994	1.64999
36	62099.7536	2.7476	62099.23720	2.23115
37	63339.3219	4.9882	63336.75704	2.42329

Numerov's method,^{4,18} as well as the present method. Outside the minimum and maximum turning points, the potential energy function is extrapolated in both methods, using

$$V(r) = c/r^{12} + d \tag{22}$$

and

$$V(r) = a/r^b, \tag{23}$$

where Eq. (22) is used to extrapolate the repulsive region ($r \leq r_{\text{min}}$) and Eq. (23) for extrapolation of the attractive region ($r \geq r_{\text{max}}$).¹⁸

We calculated the first 38 energy levels after dividing the internuclear interval from 0.45 to 3.0 Å into meshes of 637, 1274 and 2548 points. Column one in Table 3 is the vibrational quantum

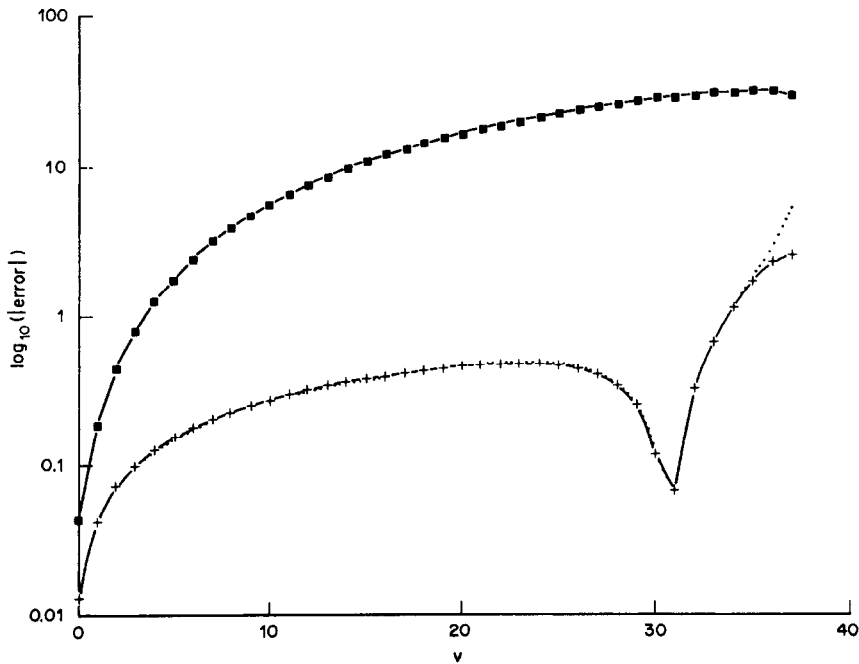


Fig. 2. The absolute errors in the derived energy levels are plotted as a function of vibrational quantum number for CO. The (■) are the errors for the calculated energy levels at a mesh of 2548 points. The (+) are the resultant errors after extrapolating to the limit using 637, 1274 and 2548 mesh points. The dotted curve shows the errors in the energy levels derived by using Numerov's method with 4459 mesh points.

number of the level. We then used the second-order extrapolation to the limit of Eq. (9) with $m = 2$ to derive the final results given in column 2 of Table 3. An estimate of the error using $R_2^{(0)}$ of Eq. (12) gives a maximum error of 0.005 cm^{-1} for the $v = 37$ level or a relative error of 7.4×10^{-7} . The difference between the extrapolated energy value and the original RKR energy is given in column 3. Again, with Numerov's method, the integration extends from 0.45 to 3.0 \AA with an interval of 0.000519 \AA for a mesh of 4459 points, the same number of mesh points we used. Column 4 presents the results obtained using the Numerov method while column 5 gives the differences between the energy levels obtained using the Numerov method and the original RKR energies. In Fig. 2, we present the errors in the CO term levels for both the present method and Numerov's method.

We see that the present method gives almost identical energy levels as Numerov's method, except for the last level. Both methods yield energy levels which start to deviate from the RKR energy levels for the vibrational levels near the points where the potential function is extrapolated by using Eqs. (22) and (23). The deviation between the RKR energy and that derived by both the extrapolated and the Numerov algorithms at the highest levels probably results from the use of analytical forms that do not match the assumptions given by Eqs. (4) and (5) that a large number of derivatives exist for the potential function near the end of the range of the original RKR derived potential function.

We have also calculated the rotational constant and compared its value with the original RKR value. The results of this comparison are given in Table 4. Columns 1–5 represent, respectively, the vibrational quantum number, v , the RKR value for the rotational constants as given in Table 4 of Ref. 5, the rotational constant calculated by using the wavefunctions derived from the Numerov method in Eq. (13), and the rotational constant calculated from Eq. (13) using the wavefunctions calculated for 2548 mesh points, and extrapolated wavefunctions derived from Eq. (9). The rotational constants calculated using the Numerov wavefunctions and wavefunctions calculated over a mesh of 2548 points are the same. However, the rotational constants calculated using extrapolated wavefunctions give results closer to the RKR rotational constants. This agreement demonstrates that the extrapolation of the wavefunctions is valid and gives better results than using wavefunctions calculated either from Numerov's method or the finite difference method without extrapolation.

CONCLUSIONS

We have presented a modification of the method of finite differences to solve Schrödinger's radial 1-D equation. The modification has been to incorporate an extrapolation procedure to obtain highly accurate energy levels and wavefunctions. This extrapolation method has a firm

Table 4. Results for the $X^1\Sigma^+$ state of $^{12}\text{C}^{16}\text{O}$; the superscripts have the following meanings: a refers to the calculation using wavefunctions with 2548 mesh points in Eq. (13); for b, calculation using wavefunctions derived from Eq. (9) in Eq. (13).

v	B_v^{RKR} cm^{-1}	B_v^{Numerov} cm^{-1}	B_v^a cm^{-1}	B_v^b cm^{-1}
0	1.9225291	1.92247759	1.92247803	1.922478203
1	1.9050225	1.90497162	1.90497017	1.904974182
2	1.8875193	1.88746914	1.88746528	1.887475569
3	1.8700196	1.86996993	1.86996248	1.869982016
4	1.8525234	1.85247468	1.85246212	1.852493696
5	1.8350306	1.83498290	1.83496490	1.835009911
10	1.7476181	1.74757367	1.74750708	1.747669839
15	1.6602918	1.66025081	1.66009077	1.660446474
20	1.5730515	1.57301025	1.57268703	1.573333360
25	1.4858973	1.48583115	1.48523269	1.486301191
30	1.3988291	1.39856861	1.39754425	1.399198893
35	1.3118470	1.31066524	1.30913472	1.311544377
36	1.2944610	1.29279922	1.29150431	1.294071757
37	1.2770783	1.27447660	1.27446920	1.277168277

mathematical foundation. Equally important are the error estimates that this extrapolation gives, which can be used to estimate the accuracy achieved. Additional attractive features of this method are that the algorithm is easy to implement and does not require initial guesses for the term values or the behavior of the slope of the wavefunctions near the minimum and maximum of the interval of integration. The method is less sensitive to round-off error than Numerov's since a small number of mesh points is used which, as a secondary result, decreases the computational time required.

Our method has been applied to finding the energy levels and wavefunctions for both an analytical potential function and a potential function derived from experiment. The present method gives better wavefunctions on a coarser mesh than Numerov's algorithm.

REFERENCES

1. D. Goorvitch, *Ap. J. Suppl.* **74**, 769 (1990).
2. C. Chakerian, Jr., R. Farrenq, G. Guelachivili, C. Rossetti, and W. Urban, *Can. J. Phys.* **62**, 1579 (1984).
3. J. W. Cooley, *Math. Computation* **XV**, 363 (1964).
4. R. N. Zare, *J. Chem. Phys.* **40**, 1934 (1964).
5. S. M. Kirschner and J. K. G. Watson, *J. Molec. Spectrosc.* **51**, 321 (1974).
6. K. P. Lawley and R. Wheeler, *J. Chem. Soc., Faraday Trans. 2* **77**, 1133 (1981).
7. P. J. Cooney, E. P. Kanter, and Z. Vager, *Am. J. Phys.* **49**, 76 (1981).
8. R. F. Boisvert, S. E. Howe, and D. K. Kahaner, *A Guide to Available Mathematical Software*, NTIS Report PB 84-171305, Springfield, VA (1984).
9. L. F. Richardson, *Trans. R. Soc. (Lond.)* **A226**, 299 (1927).
10. G. M. Phillips and P. J. Taylor, *Theory and Applications of Numerical Analysis*, Academic Press, London (1973).
11. D. G. Truhlar, *J. Comput. Phys.* **10**, 123 (1972).
12. H.-O. Kreiss, *Math. Comput.* **26**, 605 (1972).
13. H. B. Keller, *SIAM J. Numer. Anal.* **6**, 8 (1969).
14. P. Henrici, *Elements of Numerical Analysis*, Wiley, New York, NY (1964).
15. T. Håvie, *BIT* **17**, 418 (1971).
16. K. P. Lawley, *J. Comput. Phys.* **70**, 218 (1987).
17. J. K. Cashion, *J. Chem. Phys.* **39**, 1872 (1963).
18. R. N. Zare, Report UCRL-10925, University of California Radiation Laboratory, Berkeley, CA (November 1963).